Article:

Croft, Simon, Budgey, Richard, Pitchford, Jon orcid.org/0000-0002-8756-0902 et al. (1 more author) (2015) Obstacle avoidance in social groups::new insights from asynchronous models. Interface. ISSN 1742-5662

https://doi.org/10.1098/rsif.2015.0178

Abstract

For moving animals, the successful avoidance of hazardous obstacles is an important capability. Despite this, few models of collective motion have addressed the relationship between behavioural and social features and obstacle avoidance. We develop an asynchronous individual-based model for social movement which allows social structure within groups to be included. We assess the dynamics of group navigation and resulting collision risk in the context of information transfer through the system. In agreement with previous work, we find that group size has a non-linear effect on collision risk. We implement examples of possible network structures to explore the impact social preferences have on collision risk. We show that any social heterogeneity induces greater obstacle avoidance with further improvements corresponding to groups containing fewer influential individuals. The model provides a platform for both further theoretical investigation and practical application. In particular, we argue that the role of social structures within bird flocks may have an important role to play in assessing the risk of collisions with wind turbines but that new methods of data analysis are needed to identify these social structures.

Introduction

Collective motion can be observed in a wide variety of biological systems, inspiring scientists to investigate the mechanics behind such apparently complex behaviour [1–4]. Many of these studies have developed individual-based models to assess the effect of behavioural and environmental factors [5–9]. These models simulate motion through local interactions by applying rules based on proximity with individuals exhibiting three core behaviours: repulsion (avoiding collision with other individuals); orientation (aligning with nearby individuals); and attraction (movement towards distant individuals) [5, 10]. Additional rules can be incorporated to represent environmental factors, for example, navigation towards a target or response to predators [6–8, 11].

Typically, such individual-based models do not constrain the number of interactions that contribute to the motion of an individual. These are known as "metric" models, as they sum the interactions with all cues within a given distance of a focal individual [6, 7, 9]. However, empirical evidence suggests that social interactions may in fact be topological, with each individual responding only to a fixed number of other individuals [12]. Studies which develop an asynchronous updating method have demonstrated that this topological property for interactions emerges spontaneously [8]. Significant features of this modelling approach include varied speed distributions and emergent stochastic noise in the decision making process, both of which contribute to a greater degree of biological realism.

The importance of this updating scheme becomes apparent when individuals interact with other environmental factors and averaging becomes inappropriate. Of particular interest is when these environmental factors are of significant societal or conservational relevance. For example, a growing demand for renewable energy has led to a significant increase in the number of wind farm developments [13]. Wind farms are often sited in areas which intersect existing flight paths of migratory bird species, thereby forming a potential barrier to movement [14]. It is important that we understand the impact such developments could have on the level of avian mortality as a direct result of collisions in order to protect the population of at risk species [15]. There is considerable variablility in the collision risk for avian species from wind turbines, not least due to variable sampling techniques and carcass loss from scavengers, estimates for per turbine collision rates per annum span 4 orders of magnitude [15]. However, few studies in the field of collective motion have investigated the interactions of bird flocks with wind turbines or other obstacles [16, 17], primarily because of ambiguity in the methodology for incorporating obstacles (and their avoidance) within existing models.

Previous work investigating the interaction of groups with a single obstacle shows that group size has a non-linear relationship with collision risk, and that whilst initially social interactions cause a higher per capita risk of collision this is reduced with further increases [9]. This has implications for the modelling of real-world applications, especially for avian collisions where current probabilistic models [18] have no explicit dependence on group size and cannot incorporate changes in behaviour driven by social dynamics [19].

Recent studies using an asynchronous update scheme have outlined a robust framework to investigate the effect of complex behaviours such as the influence of social networks [20]. This has important applications in simulating real-world animal movement where empirical evidence suggests that both ability and influence are unlikely to be distributed evenly [21–23]. The results show that when compared to previous studies, which focus on the effects of varied ability [6, 24, 25], underlying networks representing simple examples of leadership can have a significant impact on group dynamics and navigational performance. Whilst leadership provides one example of a social network structure, other characteristics such as clustering, as a result of strong interactions between members of family groups, could also be present and have the potential to produce distinct group behaviours. This highlights the importance of identifying plausible network structures in order to produce realistic simulations of animal movements. In the case of geese such networks structures are not well established; and in pigeons it has been shown that in-flight hierarchies cannot be inferred reliably from ground-based networks [23]. Network structures in other systems are better developed, for example in humans [26], in other social animals [27] and in other application areas [28, 29].

Here, we describe an individual-based model with an asynchronous updating algorithm to investigate group interactions with obstacles. Using this model we explore the response of individuals to changes in group size. We determine the effect this may have on collision risk; initially with a single obstacles, and then with an array of obstacles representing a typical wind farm. We parametrise and then continue to simulate group interactions with an obstacle array, investigating the impact underlying social networks have on collision risk by comparing four example networks (homogeneous, random, clustered and leadership; to be defined in Methods) each representing a distinct structural characteristic. We discuss how different environmental factors may contribute to collision risk paying particular attention to the role of weather conditions, such as environmental turbulence and visibility. These factors have proved difficult to assess empirically as many studies rely upon a degree of visual observation to determine behaviour [15, 30, 31]. Finally, we investigate the trade-off between avoidance and migratory pressures such as energetic efficiency [32] by introducing a fixed straight route which group members attempt to follow, thereby minimising energy expenditure. Such behaviour imposes a previously ignored cost to obstacle avoidance which may have an important impact on predicted collision risk.

Methods

Modelling Framework

The model is adapted from the stochastic implementation outlined in [20]. Groups consist of a set of $\{1, \dots, N\}$ individuals each represented by a position $\underline{x}_i$ and a unitary heading vector $\underline{\hat{v}}_i$ in continuous two dimensional space. Inspired by computational techniques for object reconstruction, obstacles are represented by a finite set of $\{1, \dots, M\}$ vertexes and connecting edges [33]. Each obstacle vertex is represented by a position $\underline{p}_i$ and an outwardly facing normal vector $\underline{\hat{n}}_i$. By describing obstacles in this way we provide a flexible approach for approximating any shape, size or orientation without the need for complex differential geometry. The degree of error in this method can be controlled by varying the number of vertices which comprise each obstacle. This allows us to distinguish between obstacles of equal size which induce different avoidance potentials, for example as a result of varying levels of transparency. In this study we minimise the error in behavioural response by adopting a standard spacing of 1 spatial unit between vertices; provided the minimum distance used to categorise behavioural response is greater than this value individuals will detect the obstacles and react appropriately. Motivated by our wind turbine application, obstacles are considered to be transparent to the extent that they do not occlude vision.

In common with established models [5, 6, 10] an individual determines a direction of motion by responding to selected navigational cues within a given sensory zone, including migration towards a particular target. This sensory zone is defined by a circle of radius R_a centred on the individual, with an omitted blind angle β to the rear [34]. However, unlike these models, individuals are updated asynchronously according to the following algorithm:

1. Choose individual i at random.
2. Choose an "update partner" j (which may be another individual, an obstacle vertex, or the target direction) with probability P_{ij} at random from all stimuli within sensory zone (see below). If there is no stimulus then continue on current heading.
3. Determine $\underline{\hat{v}}_i$ in response to chosen partner j.
4. Update $\underline{x}_i$ and $\underline{\hat{v}}_i$.

We ensure that each individual updates on average once per time interval Δt by performing N realisations of the steps 1-4 [35]. Simulation outputs are recorded every $\tau = \lambda \Delta t$ seconds, where λ (≥ 1) defines the average number of updates performed by each individual. When $\lambda > 1$ the resulting behaviour between consecutive model outputs is the sum over a number of updates [20]. The choice of λ is discussed in table 1.

The probability of an individual selecting a particular update partner is initially weighted based on the type of interaction. Interaction weighting are defined as social (w_s), obstacle (w_o) and target (w_t). Each of these weightings is modified according to a spatial relationship providing distinction between partners of the same type. Social and obstacle interactions are each scaled by a factor equal to the inverse of relative distance ($d_{ij} = |\underline{x}_j - \underline{x}_i|$); capturing the averaged effect of visual occlusion. In addition, obstacle vertices which appear outside of the frontal region defined by a sector of angle α and radius greater than $R_r{}^o$ are considered to have a weighting of zero.

In order to emulate the effect of social networks within the group we construct an underlying fixed matrix with elements e_{ij} (≥ 0). This matrix remains unchanged through the simulation and contains information on the long-term social preference and bonds between group members. The factor $\epsilon_{i,j}$ further scales the probability of an individual i selecting a particular neighbour j. The details and implications of this methodology are discussed in detail elsewhere [36, 37].

Finally, the weighting for target navigation comprises two parts, a constant directional part (w_{t0}), and a variable part (w_{t1}) which is determined by a function of the angle between the individuals current heading and its ideal target direction (ϕ). As an individual orientates away from its ideal target heading this angle becomes greater, increasing the target selection weighting. This simulates a desire for group members to follow a particular route with strong route fidelity, a well established trait of migratory birds (e.g. [38]). In summary, for an individual i in a group with individuals $n = \{1, .., N\}$ augmented with the obstacle vertices $m = \{1, .., M\}$ and the target, then update partner $j \in \{1 + N + M\}$ is chosen with probability:

$$P^s_{ij} = (\frac{w_s e_{ij}}{d_{ij}})w^{-1}, \quad P^o_{ij} = (\frac{w_o}{d_{ij}})w^{-1}, \quad P^t_{ij} = (w_{t0} + w_{t1}(1 - \cos(\phi))w^{-1}$$

where w is the sum of weighting for all stimulus. P^s_{ij}, P^o_{ij}, P^t_{ij} denote the probabilities for social, obstacle and target interactions respectively. It is important to note that this differs from previous implementations of this model [20] which use a constant probability for the target; here the target is merged into the pool of update partners that can occur at each micro-step, and as a result the target preference is dependent upon the weight of other stimuli.

Once a partner has been selected, the updating individual must determine how to respond according to the type of update partner. If a neighbour is selected, then the focal individual's sensory zone is divided into hierarchical interaction zones of radius ${R_r}^s$, ${R_o}^s$ and R_a which dictate whether repulsion, orientation or attraction manoeuvres are performed respectively. Here, attraction manoeuvres are applied with a velocity of $2v_0$, representing the increased thrust required by an individual to reduce their distance to neighbours, maintaining group cohesion. Similarly, if an obstacle vertex is selected a repulsive manoeuvre is applied within a zone of radius ${R_r}^o$. For any vertices which appear at a distance greater than ${R_r}^o$ we apply a pre-emptive avoidance strategy equivalent to social alignment which aims to limit more extreme repulsive action. Previously, it has been proposed that individuals should attempt to align themselves with the surface of an obstacle at the point of interaction [9]. For birds, which have been shown to have largely monocular vision [17], this type of information requires a degree of depth perception that is likely to be beyond their sensory capability. Instead, in this model we suggest a simpler response where individuals turn away from obstacle vertices to maintain a minimum angle of α between their heading and the trajectory intersecting the vertex. The cumulative effect of this response results in an individual attempting to avoid an obstacle on a trajectory which requires the least deviation from its current heading.

If target navigation is selected then an individual aims for a point that is a fixed distance (d_t) from its current projected position along the group target trajectory, inspired by route fidelity found in other species. This target trajectory is defined by the straight line starting at the initial group centre of mass and continuing indefinitely in the direction specified by a fixed target vector ($\hat{\underline{v}}_t$). This implements instantaneously perfect navigation on a linear route. Other studies have considered error in navigation [7], but when this variation is introduced into the model presented here it is dominated by the inherent noise in the underlying algorithm [39]. For the application to collision avoidance, navigation error is therefore of less importance then some of the other features varied in our analysis.

To represent the finite ability of an individual to execute a turn in the direction of its preferred heading, we implement a maximum turning rate of θ. In simulations which apply a movement error to represent environmental turbulence we rotate the calculated heading vector, following the application of a turning limit, by an angle randomly drawn from a Von Mises distribution with mean of zero and equivalent standard deviation w_e. Intersections with obstacles are recorded when the trajectory of an individual intersects either an obstacle vertex or connecting edge. In this implementation of the model we consider the probability of these intersections resulting in a fatal collision to be zero. Consequently, intersecting individuals are not removed from simulations.

We compute various metrics to summarise the data from our simulations. **Target navigation ability** is defined as the fraction of the trajectory that all birds spend travelling to the target direction. This is computed as the dot product of the mean group direction with the target direction, scaled by the mean distance traveled, averaged over the simulation. The **probability of splitting** is computed by calculating the fraction of simulations which contain more than one group at a fixed time period after passing the line $y = 0$. This include both spontaneous splitting and interaction with the obstacle to enable a measure of relative disruption to be computed. The number of groups is calculated using an equivalance class relation with the equivalence based on the radius of alignment. The **probability of avoidance** is computed by averaging the number of individuals which intersect a single wind turbine (micro) or array of wind turbines (macro) across all independent simulations of a given scenario. The latter measure is utilised in all except figure 2(a), as noted in the captions.

Parameterisation

Parameters are chosen to nominally represent flocks of pink-footed geese (*Anser brachyrhynchus*) interacting with an array of wind turbines. Where possible parameter values have been taken from empirical data. Time and space steps, and model parameters, are related to their real world units and values in Table 1. Following [40] the width of obstacles used in simulations is fixed at 100 metres, which represents a typical offshore wind turbine.

In simulations where we investigate the effect of heterogeneity in the abilities of group members, the values of obstacle avoidance and target preference are varied. For each individual the parameters stated in table 1 are scaled by a value randomly selected from a normal distribution with mean equal to 1 and standard deviation w_h, which provides a quantification for heterogeneity.

In order to simulate underlying social networks we define interaction matrices with elements e_{ij} denoting the strength of the social connection individual i has towards neighbour j. For a **unitary homogeneous network** we consider connections between neighbours to have a weight equal to 1 ($e_{ij} = 1$). Connections between the same individual are disallowed ($e_{ii} = 0$). **Random networks** are generated relative to this unitary matrix so as to maintain a balance between the average weight of all detected social interactions relative to obstacle and target interactions. Initially, we assume that all individuals are at least weakly connected with weight w_n. Connections are selected at random and incremented by w_n until the sum of all elements is equal to that of the homogeneous case.

For **clustered and leadership networks** the connections which can be incremented are limited to a specific subgroup. In the case of a leadership network l individuals are randomly identified as leaders. The only matrix elements which can be incremented are those which describe the connections from a remaining group member to any of these leaders. In the case of clustered networks, group members are assigned a number between 1 and c representing a fixed number of subgroups. The only matrix elements which can be incremented are those which describe the connections between group members with matching cluster index. Unless otherwise stated simulations use a unitary homogeneous network.

Simulations

Simulations consist of two phases: an initial warm up, followed by a phase of interaction with obstacles. Each phase is performed for a period of 1000 time steps in an unbounded environment. The warm up phase allows groups to form a representative configuration in the absence of obstacles. Here, we define a representative configuration to mean that all individuals belong to an equivalence class where neighbours are declared equivalent if they are within a distance equal to the radius of alignment (${R_o}^s$). Thereby, each individual must as a minimum be in a position to align with at least one neighbour. It should be noted that individuals can become permanently separated from the main group. In such cases where a representative configuration is not formed the warm up phase is repeated.

The group is then reset with its centre placed on a selected origin and rotated so that the average heading is equal to the specified target direction. In simulations with a single obstacle we use a fixed origin which is located 5000 metres from the obstacle centre in the target direction. Otherwise, groups interact with an array containing 25 obstacles uniformly arranged on a square grid at 500 metre intervals, the representative spacing of wind turbines [44].

To focus on behavioural effects and minimise the effect of starting conditions we perform the following randomisation scheme on the initial positions. The origin is randomly selected on a line segment with midpoint 6000 metres from the array centre (approximately 5000 metres from the nearest obstacle) in the target direction and extending perpendicular to this vector. The group centre may be placed either side of the segment midpoint at a distance corresponding to the cross-sectional width of the obstacle array excluding a 50 metre buffer zone at both ends. This guarantees that, if there is no avoidance behaviour, individuals will intersect the area bounding the array. By varying the origin of groups we sample all potential interactions with the array. To minimise the number of direct routes through the array we offset the angle of approach, between the target direction and the orientation of columns in the array, by 12 degrees, at which the probability of an individual avoiding all obstacles without evasion is negligible.

Once the simulation warm up phase is complete, the phase of obstacle interaction is initiated, during which individual level trajectory data is recorded at discrete time intervals (τ). For each set of parameters we per-

Symbol	Value	Description and Unit (where appropriate)
N	30	Number of individuals within the group [9].
τ	1	Time interval for each individual to perform, on average, λ updates (in seconds) [8, 20].
Δt	0.01	Time interval for each individual to perform, on average, a single update step (in seconds) [8, 20].
λ	100	Update frequency represents the average number of updates an individual performs per second [8, 20, 41].
v_0	15	Average cruise speed in metres s^{-1} [32].
α	45	Angle of pre-emptive obstacle avoidance needed to observe a minimum distance of ${R_r}^o$ from vertexes.
β	60	Angle of rear blind region of an individual (in degrees) [34].
θ	80	Maximum horizontal turning rate (degrees s^{-1}) [32].
${R_r}^s$	2	Radius of social repulsion, in metres, representing the average size of an individual, in this case the wingspan [32].
${R_r}^o$	150	Radius of obstacle repulsion, in metres, average minimum distance maintained by individuals from obstacles, in this case geese from wind turbines [30].
${R_o}^s$	20	Radius of social alignment, in metres, maximum nearest neighbour distance within groups, in this case flocks of geese [42].
R_a	1000	Radius of attraction, in metres, representing the maximum perception distance of an individual, in this case the maximum distance from wind farms which geese show avoidance action [43].
w_s	1	Social preference weighting, the priority an individual shows towards selecting a neighbour for an "update partner".
w_o	1	Obstacle avoidance weighting, the priority an individual shows towards selecting an obstacle vertex for an "update partner".
w_t	0.1	Target preference weighting, the priority an individual shows towards selecting the target for an "update partner".
w_{t0}	0.1	Baseline target preference weighting, the minimum weighting which guarantees successful navigation towards a designated target.
w_{t1}	0	Variable target preference weighting, the coefficient which scales the maximum target preference weighting.
w_n	0.1	Network weighting, the magnitude of increments applied to interaction matrix elements used in random network generation.
w_h	0	Heterogeneity, the standard deviation of the normal distribution used to vary avoidance and target preferences between individuals.
d_t	30000	Target heading distance, defines the distance along group target trajectory which an individual navigates towards. This is chosen to minimise the lateral effect on group structure.

Table 1: List of parameters used in model simulations. Values stated are for a typical group interacting with a square array of 25 obstacles. Where appropriate, physical parameters have been set based on values from existing empirical studies.

form 100 iterations and using this trajectory data calculate the statistics characterising group dynamics and collision risk.

Results

Prior to introducing any obstacles, the first step is to establish what baseline target preference is necessary for the model to reproduce the observed biological phenomenon of coherent group navigation along a nominated trajectory. Figure 1 summarises this process: Panel (a) confirms that the minimum target preference required, relative to a social weighting of unity, is approximately 10^{-2}; Panel (b) shows that group cohesion is initially improved by a common navigational direction but that there exists a maximum baseline target preference of approximately 10^{-1}, above which relative social preference is insufficient to maintain group cohesion. Combining these results we identify this maximum threshold as an appropriate value for baseline target preference across all group sizes. In addition to the results shown in figure 1 we observe that mean nearest neighbour distance decreases as a function of group size, consistent with Hemelrijk and Hildenbrandt [45].

We can now begin to explore the effect of avoidance preference in relation to collision risk (Figure 2). In common with a simpler fixed time step model [9], we find that avoidance is dependent upon group size, with smaller groups displaying an increased ability to avoid both single obstacles and arrays across all parameter values. Furthermore, it can be seen in figure 7 that this relationship can be non-linear. In the context of avian interactions with wind turbines we aim to identify a suitable parameter value for avoidance preference by comparing the data in figure 2(b) to estimated wind farm avoidance rates for migrating geese. This plot shows a sharp improvement in avoidance around a value of 1 with an average probability of avoidance across all group sizes reaching approximately 60%. This lies well within the range of estimates for wind farm avoidance observed by empirical studies which record values between 50 and 70% [46]. Empirical studies also observe that of the remaining individuals which enter the wind farm area more than 99% successfully avoid all wind turbine structures resulting in an overall avoidance rate of approximately 99.8% [31, 47]. However, it should be noted that there are some studies which record 100% avoidance [30] – for our chosen value of $w_o = 1$ individuals entering the array are able to successfully avoid all obstacles.

Using the parameter values identified above for all subsequent simulations we explore the effect that heterogeneity within a group has on collision risk.

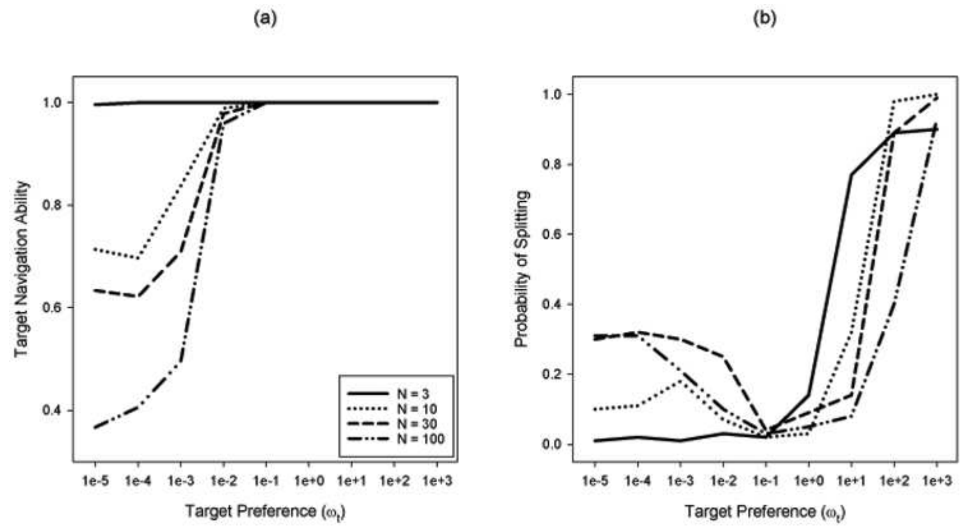

Figure 1: Parametrising target preference for coherent directed groups. For social groups ($w_s = 1$) of varying size (N) in an obstacle-free environment, we plot: (a) average proportion of distance travelled parallel with target trajectory; (b) probability of a group splitting; (recorded after 1000 time steps) as a function of baseline target preference (w_{t0}). We observe that beyond a critical value ($0 < w_t \leq 0.1$), dependent on N, navigation occurs directly along the target trajectory. This common direction appears to improve group cohesion reducing the probability of splitting but as w_{t0} increases further social preference is overwhelmed resulting in an increased proportion of groups splitting.

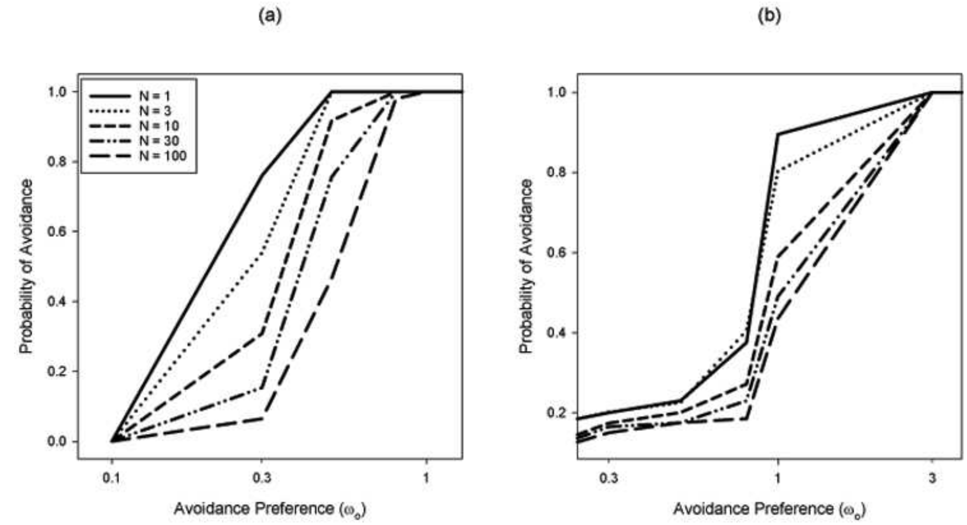

Figure 2: Avoidance of an obstacle does not guarantee avoidance of an array. For social groups ($w_s = 1$) of varying size (N) and baseline target preference ($w_{t0} = 0.1$) we plot the probability of avoiding the region bounding an array containing: (a) a single obstacle; (b) 25 obstacles uniformly arranged on a square grid at 500 metre intervals; (recorded after 1000 time steps) as a function of avoidance preference (w_o). For each, group target trajectory intersects the array at an angle which minimises the probability of avoiding all obstacle given no avoidance behaviour. As expected the probability of avoidance increases with w_o. However, this relationship is not linear but instead shows a sharp step at a critical value of preference particularly evident in (b). In common with previous studies [9] there appears a dependence upon N, with smaller groups displaying a higher propensity for avoidance. We note that the probability of avoiding all obstacles in case (b) (not shown) is qualitatively similar to (a) with transitions appearing at marginally lower values of preference. Consequently, groups demonstrate total avoidance of all obstacles in (b) prior to any avoidance of the array as a whole.

In particular, we exploit the potential of an asynchronous update scheme to implement varying types of underlying social networks which may influence group decisions.

Figure 3 shows that different network structures have distinct effects on both the probability of avoiding an obstacle array and the resulting group structure. We see that groups which navigate according to a homogeneous network show the least ability to avoid obstacles, but demonstrate little disruption to group structure (measured by the probability of the group splitting). Comparing subsequent groups to this benchmark we notice that any degree of heterogeneity within a network produces a higher probability of avoidance, but that this can be at a cost to group cohesion. This is most notably the case for leadership groups, which demonstrate the highest probability of avoidance but also a high probability of splitting. For these groups we see that avoidance is related to the number of leaders, with fewer influential individuals providing the highest levels of avoidance. The number of leaders does not affect splitting, which remains high. Clustered groups appear to follow a pattern similar to that seen for group size. Here, as the degree of clustering is increased, thus reducing the number of individuals per cluster, we observe an increase in avoidance. This is matched by an increase in the probability of splitting suggesting that clusters may begin to act independently as their size is reduced.

For all networks the probability of avoidance shows a bimodal distribution in that, for a given simulation, either all group members traverse the array, or all successfully avoid the array. This is of particular significance when considered with figure 4 which maps the trajectories of groups responding to the array. Despite varying probabilities of avoidance we see only marginal differences between movement patterns. This suggests that avoidance is limited by the ability of a group to initiate an avoidance response rather than an ability to perform the action. The horizontal trajectories seen for leadership networks (panel (d)) are likely due to a loss of contact with the lead individual during separation. A lower preference for other group members increases the probability of separations becoming permanent resulting in this self-navigation through the array.

Motivated by previous studies [6, 24], we then introduce groups which contain individuals with heterogeneous abilities, in this case the preference for avoidance and target navigation, i.e. $(w_o)_i = w_o + w_h * N(0,1)$ and similarly for the target weighting for each individual i. The results shown in figure 5 demonstrate that as the magnitude of heterogeneity is increased groups experience an increased disruption to group cohesion and reduced probability of avoidance. This suggests that the relative variation of avoid-

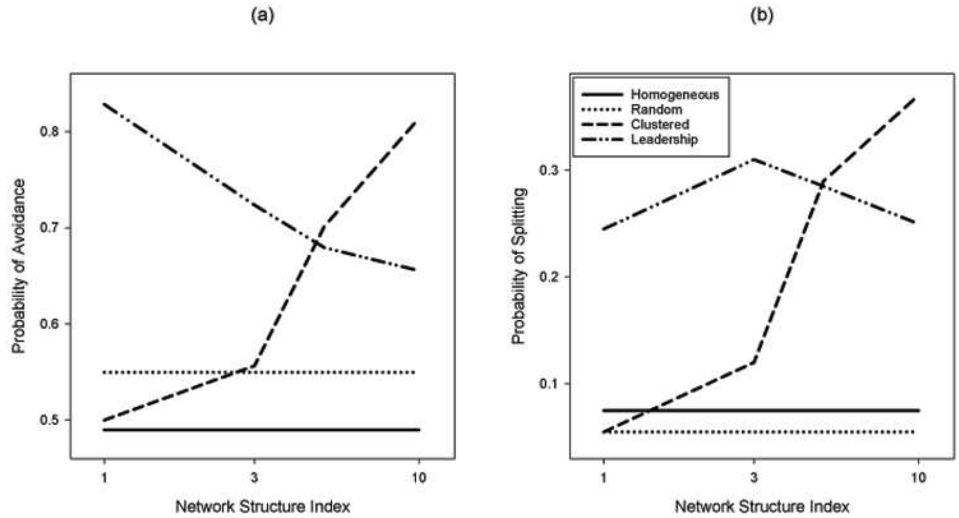

Figure 3: Heterogeneous social structure promotes obstacle avoidance. For social groups ($w_s = 1$) of 30 individuals with baseline target preference ($w_{t0} = 0.1$) and avoidance preference ($w_o = 1$) intersecting an array containing 25 obstacles uniformly arranged on a square grid at 500 metre intervals, we plot: (a) probability of avoiding a region bounding the array; (b) probability of a the group splitting; (recorded after 1000 time steps) for various examples of underlying social network (homogeneous, random, clustered and leadership), as a function of network structure index indicating the precise number of clusters or leaders in respective network types (homogeneous and random networks are invariant). We observe that homogeneous groups display the least avoidance ability, generally followed by random networks. Clustered networks produce increasing avoidance and splitting with the number of clusters. Groups which employ a single leader exhibit the highest levels of avoidance but as the number of leaders increases avoidance is reduced.

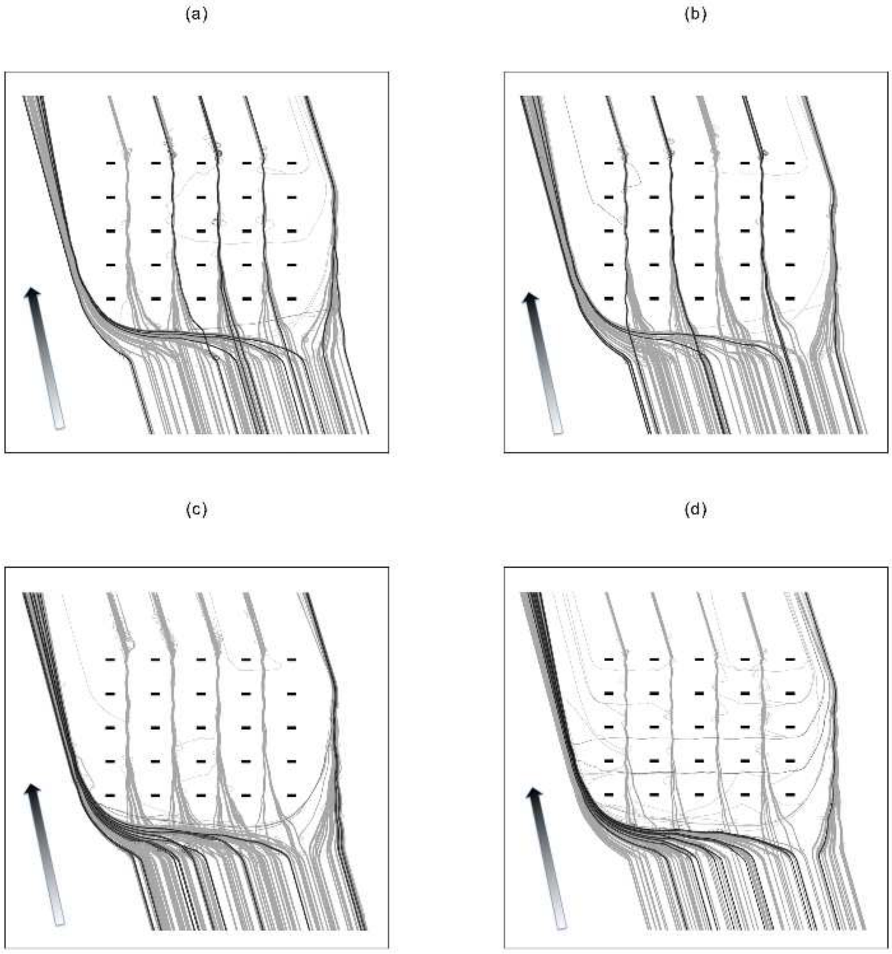

Figure 4: Similar movement patterns for distinct network structures. Mapped trajectories for groups with baseline target ($w_{t0} = 0.1$) and avoidance preference ($w_o = 1$) intersecting an array which contains 25 obstacles uniformly arranged on a square grid at 500 metre intervals and: (a) homogeneous; (b) random; (c) clustered; (d) leadership; underlying network structures. Each plot displays trajectories for 100 groups (light grey) of 30 individuals. 10 groups are highlighted (dark grey) with a focal individual (black). In (d) this focal individual represents the group leader. These plots can be compared to empirical data presented in [44]. We observe similar patterns of movement for all networks with only marginal differences in coherence ((b) shows less splitting) and cohesion ((c) shows high and (d) low density reflecting neighbour distances). See also supplementary movies S1a - S1d, corresponding to the panels in this figure.

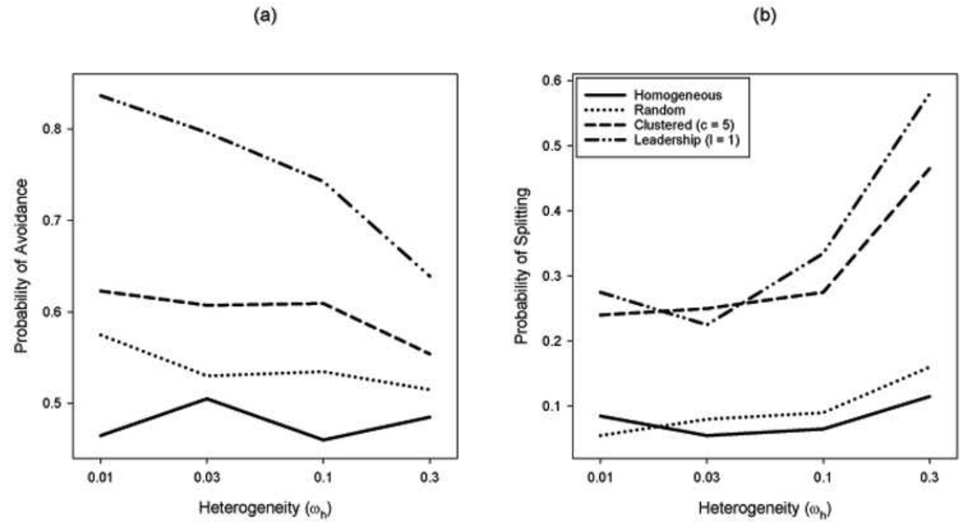

Figure 5: Variable ability reduces avoidance and group cohesion. For social groups ($w_s = 1$) of 30 individuals with baseline target preference ($w_{t0} = 0.1$) and avoidance preference ($w_o = 1$) intersecting an array containing 25 obstacles uniformly arranged on a square grid at 500 metre intervals, we plot: (a) probability of avoiding a region bounding the array; (b) probability of a the group splitting; (recorded after 1000 time steps) for various examples of underlying social network (homogeneous, random, 5 clusters and a single leader), as a function of heterogeneity w_h (magnitude of variation in avoidance and baseline target preferences). We observe that groups with a single leader are the most affected by changing heterogeneity showing a decrease in avoidance and increase in splitting as abilities become more variable. Clustered networks also induce this pattern although it is less pronounced. Groups with homogeneous and random networks appear largely unaffected by changes in heterogeneity showing only at small increases in splitting at high levels.

ance and target preferences alters the balance towards target navigation. In general, we see that groups which rely on fewer individuals for navigational decisions are more affected by this variation.

In order to assess whether the collisions observed by empirical studies could be explained by an increased risk as a result of environmental conditions, we vary the magnitude of movement error and the radius of attraction, the limit of an individuals sensory zone, to simulate turbulence and visibility respectively. Figure 6 shows that in both cases as parameters are varied to simulate poorer environmental conditions groups which rely on a particular individual for navigation are significantly influenced, transitioning from showing the most avoidance to the least. In the case of turbulence this result contradicts [7], which shows asocial groups navigate more effectively in variable environments than their social counterparts. However, the trajectories mapped in panel (b)(i) (when compared with figure 4(a)) support the idea that at least for social groups, target navigation is significantly affected by turbulence. In highly turbulent environments groups are less likely to follow the target trajectory intersecting the array, and so appear to improve their ability to avoid obstacles. For those groups which are able to maintain accurate target navigation, such as those which rely on a particular individual, we have clear evidence that avoidance behaviour is susceptible to poor conditions. Our simulations suggest that in all groups environmental conditions affect avoidance behaviour, but the response is dependent on the social structure. The increased dependence on local decisions makes it less likely that the groups will enter the array but the effect of this is to cause greater disruption to the group which may have significant effects on other fitness costs not captured here.

Despite the erratic movements of groups in turbulent environments (panel (b)(i)), individuals retain the ability to avoid obstacles and we observe no collision risk for any level of turbulence. This is not the case in environments which simulate low visibility. We find that, as visibility is reduced, group show much later and more extreme avoidance responses resulting in the stepped movement patterns in panel (b)(ii). Here, we see that for some groups the loss of pre-emptive avoidance means they are no longer able to react in time to prevent intersections with obstacles.

Finally, we investigate the effect of introducing a variable target preference simulating the desire of groups to follow a direct migratory route with high fidelity. This is implemented by an allowing an increase in selection of an individual when the local angular deviation from the route increases. For comparison we parametrise the component of variable target preference such that with an inflated avoidance preference of $w_o = 3$ the avoidance rate for a group of 30 individuals is equivalent to the typical case. It should be noted that the use of a variable target preference with this parametrisation does not alter the results seen for groups in obstacle-free or single obstacle environments. The plot in figure 7(a) shows that this need for route fidelity significantly alters the relationship between avoidance and group size, reversing the trend from non-linearly decreasing with group size to show a marginal increase. The change in avoidance is most noticeable for smaller groups which show a reduction in avoidance whereas the values for larger groups remain relatively unchanged. In comparison with groups which apply no cost to avoidance, the mapped trajectories shown in panel (b) show that,

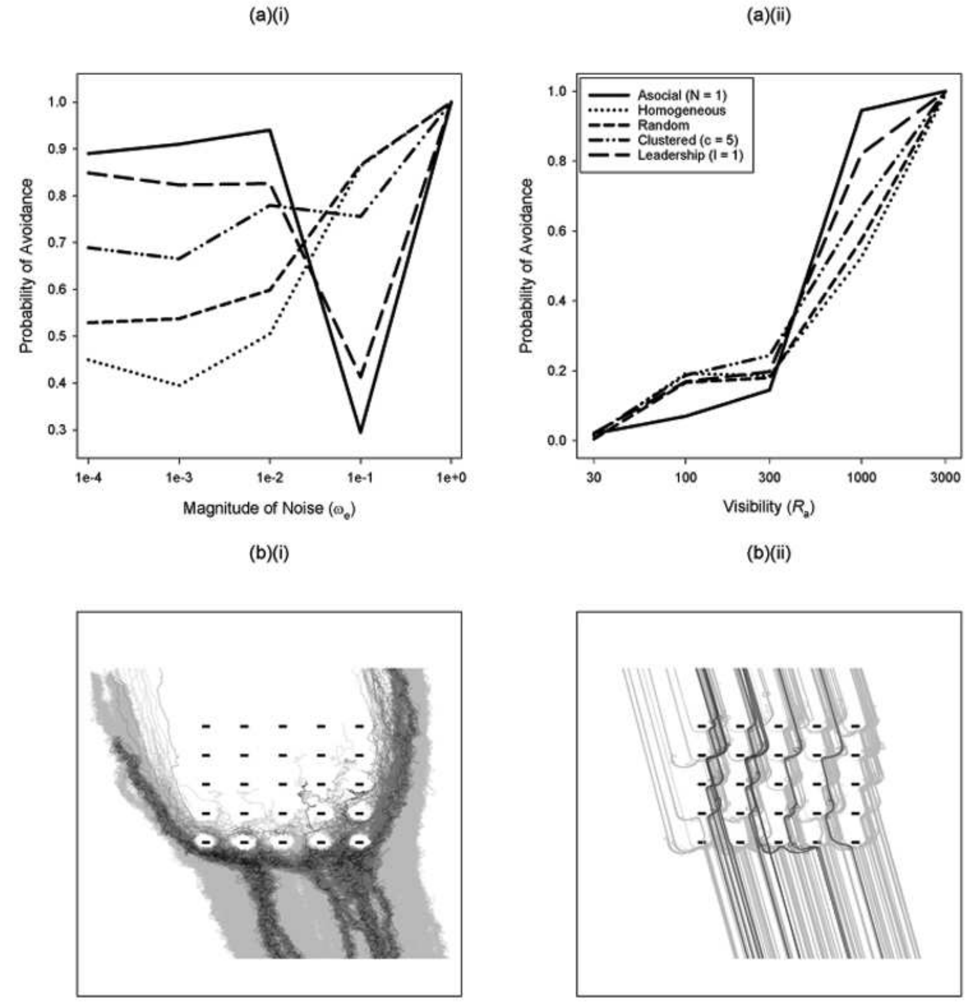

Figure 6: Leaderless groups appear less susceptible to environmental factors. For social groups ($w_s = 1$) with baseline target preference ($w_{t0} = 0.1$) and avoidance preference ($w_o = 1$) intersecting an array containing 25 obstacles uniformly arranged on a square grid at 500 metre intervals, we plot: (a) probability of avoiding a region bounding the array (recorded after 1000 time steps) as a function of: (i) turbulence (w_e); (ii) visibility (R_a); for various social structures; (b) trajectories for 100 groups of 30 individuals (light grey) with underlying homogeneous network in an environment where: (i) $w_e = 0.1$ (increased from 0); (ii) $R_a = 100$ (decreased from 1000). 10 groups are highlighted (dark grey) with a focal individual (black). Groups with a leader initially display the most avoidance but as conditions worsen they transition to showing the least. Mapped trajectories show that when visibility is reduced collisions can occur.

despite evidence indicating an earlier initiation of avoidance, the response is limited by the increased route fidelity. Consequently, groups are much less likely to avoid the array when required to travel across the corridors between columns of obstacles.

Discussion

We have outlined a method by which obstacle interactions can be incorporated into an asynchronous individual-based model without compromising biological realism. The novel mechanism by which our model balances social and navigational forces creates a trade-off between group interactions and responses to environmental cues. Social interactions are dependent not only on social preference but also relative distance, meaning that groups with decreased nearest neighbour distance will exhibit more social tendencies. When individuals interact socially they pass on indirect information about environmental cues. This information is necessarily 'noisy', but averaging across multiple neighbours can filter noise [7]. A complementary study [48] shows that the noise experienced by individuals can have an important role on group dynamics in the presence of obstacles – where this noise is small, the group may be too inflexible to adjust to the presence of obstacles and maintain cohesion.

For environmental cues, such as target navigation, where the directional information is similar for all group members, averaging provides a robust method by which individuals can combine knowledge to formulate a cohesive group response. However, when individuals are subject to conflicting information averaging can result in an inappropriate group decision, as can be case for obstacle avoidance where response is highly dependent upon spatial position. This is of particular relevance where the ideal avoidance strategy is unclear, for example when an obstacle is spaced equally either side of the group centre. In such situations the movements of an informed individual or cluster can sufficiently influence group decisions to initiate a successful avoidance response [6] and break the decision deadlock [49]. This is consistent with our results for varied group sizes which show an increase in avoidance for groups comprising fewer individuals. Here, average information is obtained across a smaller sample thus allowing for a greater bias from particular individuals, with leaders emerging more frequently. When information cannot be resolved to achieve a unified group decision this results in the formation of localised subgroups which overwhelm the social bonds holding the group together and separate away in a different direction.

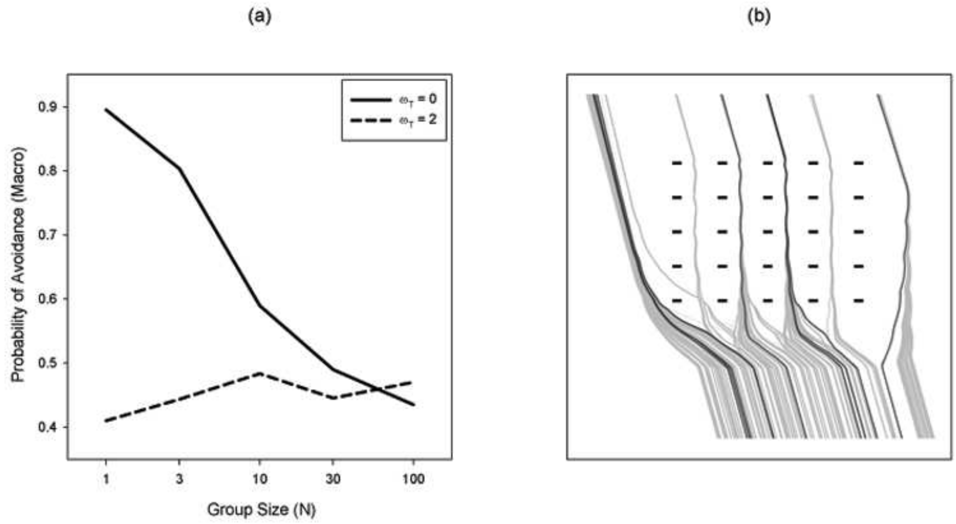

Figure 7: Route fidelity outweighs collision risk for small groups. For social groups ($w_s = 1$) with baseline target preference ($w_{t0} = 0.1$) intersecting an array containing 25 obstacles uniformly arranged on a sEnergetic benefitquare grid at 500 metre intervals, we plot: (a) probability of avoiding a region bounding the array (recorded after 1000 time steps) for different sets of avoidance and variable target preference ($w_o = 1$, $w_{t1} = 0$ and $w_o = 3$, $w_{t1} = 2$), as a function of group size (N); (b) trajectories for 100 groups of 30 individuals (light grey) with avoidance ($w_o = 3$) and variable target preference ($w_{t1} = 2$). Groups with no consideration for route fidelity show a non-linear relationship where avoidance decreases with group size. When an cost to avoidance, due to a lack of fidelity, is introduced the relationship with group size is reversed. Mapped trajectories show few avoidance manoeuvres which cross multiple corridors between columns. Groups are most likely to traverse the array along the nearest corridor in the target direction. Exceptions occur when this is an outer corridor with groups instead choosing to navigate outside the array.

Our results show that underlying social networks produce significant differences to both group structure and navigational response. When compared with the leaderless homogeneous case described above, we find that for any underlying networks where preference is shown towards interactions with particular individuals, groups demonstrate a higher probability of avoidance. This is consistent with the similar improvements shown elsewhere [50]. This behaviour results from an increased bias within the group decision making process. Consistent with existing studies we observe that groups with fewer influential individuals provide the most effective response to contradictory environmental information [24]. In contrast with this type of leadership, examples which simulate clustering show the emergence of smaller independent groups showing less cohesion but maintaining an ability to initiate avoidance actions without clearly defined leaders.

Whilst a reliance upon fewer individuals for navigation can be beneficial it is also less robust to sensory variability [7]. When variation is applied to both target and avoidance preferences the ability of such individuals to lead a group may not justify the influence which neighbours show towards them resulting in impaired navigational responses. Conversely, we find that when movement error is applied to simulate turbulence groups which navigate either asocially or with a single leader maintain coherent target navigation even in highly disruptive environments. Unlike in Codling et al. [7] where this result represents a positive outcome, in our model avoidance ability is not maintained at a relative level and whilst other groups avoid the array as a result of inaccurate navigation those which maintain target navigation consequently intersect the array more frequently. However, it is clear that even at high turbulence individuals maintain a safe distance from obstacles which suggests in our chosen parameter range that the risk of collision is effectively zero. This is not the case when the sensory range of individuals is reduced, mimicking conditions of poor visibility 7. Collisions are observed when the sensory range falls below the radius of obstacle repulsion thus reducing the distance in which individuals have to respond to initiate an avoidance manoeuvre.

Throughout this study we have assumed that collision rates are the result of deficiencies in sensory ability. We challenge this assumption by suggesting that all groups may in fact posses an ability to avoid obstacles but instead choose to enter arrays because of strong route fidelity related to migratory efficiency. By introducing a variable element to target preference which produces an increasing desire to select target navigation as individuals deviate further away from the optimal target trajectory, we show that groups containing fewer individuals are much more likely to voluntarily enter the array.

This has potentially important consequences for groups that are weakened, for example by lack of food, and may make different times of the year more important for collision vulnerability.

The ultimate goal of this modelling study is to quantify the risk of avian collisions with wind turbines. We recognise that at present the model outlined here is limited to specific scenarios in which individuals show no vertical avoidance. In reality, large-scale studies suggest that in good conditions birds, such as geese, favour vertical avoidance. Our modelling methods are amenable to generalisation to three-dimensions [31] where data are available. However, through simulations with an array containing multiple obstacles we demonstrate that the cumulative avoidance response to those obstacles is sufficient to produce movement patterns which can be compared to those recorded by empirical studies. We show that by selecting reasonable parameter values we can reproduce estimated avoidance rates. Furthermore, we use the model to explore conditions which are difficult to assess empirically. These results reinforce the suggestion that birds are most at risk of collision when conditions reduce detection distance, for example during nocturnal navigation.

The effect of social networks has not previously been modelled in the context of obstacle avoidance. We have shown in this study that social interactions can affect the ability of a group to perform suitable avoidance responses and it would therefore be ecologically informative to include realistic social networks when assessing risk. The structure of networks has been shown to have considerable impact on group behaviour, in ecological examples [6, 36] as well as in other biological settings [51]. Compared with our simple examples, goose social networks have been shown to be more complex and highly variable [21, 22]. The relationship between in-flight communication networks and important social structures, such as foraging groups or family grouping, has been shown to have complex correlations which make it difficult to interpolate between them [23]. Therefore, caution must be exercised in making social inferences from in-flight interactions and consequences. Our results indicate that movement patterns, similar to those obtained by current radar studies which assess collision risk, cannot be used to infer the structure of social networks. This observation highlights the need for greater focus on the motion of individuals in the context of obstacle avoidance. To address these deficiencies new experimental approaches are necessary so that individual-based social network models can be verified and utilised to their full potential to predict avoidance rates *in silico*. With these advances it may be possible to inform decisions regarding the impact on birds prior to the construction of wind farms.

Acknowledgments

This work was supported by the Animal Health and Veterinary Laboratories Agency (AHVLA) and jointly funded by the University of York and the Food and Environment Research Agency (FERA) through a Department for Food, Environment and Rural Affairs (DEFRA) Seedcorn grant.

References

[1] Aoki, I., 1982. A simulation study on the schooling mechanism in fish. Bull. Jap. Soc. Sci. Fish 48, 1081–1088.

[2] Major, P., Dill, L. M., 1978. The three-dimensional structure of airborne bird flocks. Behavioural Ecology and Sociobiology 4, 111–122.

[3] Heppner, F. H., 1997. Three-dimensional structure and dynamics of birds flocks. In: Parrish, J. K., Hamner, W. M. (Eds.), Animal Groups in Three Dimensions. Cambridge University Press, UK, pp. 68–89.

[4] Czirok, A., Vicsek, T., 2001. Collective motion. In: Vicsek, T. (Ed.), Fluctuations and Scaling in Biology. Oxford University Press, UK, pp. 177–242.

[5] Couzin, I. D., Krause, J., James, R., Ruxton, G. D., Franks, N. R., 2002. Collective memory and spatial sorting in animal groups. Journal of Theoretical Biology 218, 1–11.

[6] Couzin, I. D., Krause, J., Franks, N. R., Levin, S. A., 2005. Effective leadership and decision making in animal groups on the move. Nature 433, 513–516.

[7] Codling, E. A., Pitchford, J. W., Simpson, S. D., 2007. Group navigation and the many-wrongs principle in models of animal movement. Ecology 88, 1864–1870.

[8] Bode, N. W., Franks, D. W., Wood, A. J., 2011. Limited interactions in flocks: relating model simulations to empirical data. Journal of The Royal Society Interface 8, 301–304.

[9] Croft, S., Budgey, R., Pitchford, J. W., Wood, A. J., 2013. The influence of group size and social interactions on collision risk with obstacles. Ecological Complexity 16, 77–82.

[10] Reynolds, C. W., 1987. Flocks, herds and schools: A distributed behavioral model. SIGGRAPH Comput. Graph 21, 25–34.

[11] Inada, Y., Kawachi, K., 2002. Order and flexibility in the motion of fish schools. Journal of Theoretical Biology 214, 371–387.

[12] Ballerini, M., Cabibbo, N., Candelier, R., Cavagna, A., Cisbani, E., Giardina, I., Lecomte, V., Orlandi, A., Parisi, G., Procaccini, A., Viale, M., Zdravkovic, V., 2008. Interaction ruling animal collective behavior depends on topological rather than metric distance: Evidence from a field study. Proceedings of the National Academy of Sciences 105, 1232–1237.

[13] UK Renewables, November 2013. http://www.bwea.com.

[14] Masden, E. A., Reeve, R., Desholm, M., Fox, A. D., 605 Furness, R.W., Haydon, D. T., 2012. Assessing the impact of marine wind farms on birds through movement modelling. Journal of the Royal Society Interface 9, 2120–2130.

[15] Drewitt, A. L., Langston, R. H. W., 2008. Collision effects of wind-power generators and other obstacles on birds. Ann N Y Acad Sci. 1134, 233–266.

[16] Banks, R. C., 1979. Human-related mortality of birds in the united states. Tech. rep., Washington, DC: US Fish and Wildlife Service, Special Scientific Report.

[17] Martin, G. R., 2011. Understanding bird collisions with man-made objects: a sensory ecology approach. Ibis 153, 239–254.

[18] Band, W., Madders, M., Whitfield, D. P., 2005. Developing field and an521 alytical methods to assess avian collision risk at wind farms. In: Lucas, M. D., Janss, G., Ferrer, M. (Eds.), Birds and wind power. Lynx Edicions, Barcelona, Spain, pp. 259–275.

[19] Chamberlain, D. E., Rehfisch, M. R., Fox, A. D., Desholm, M., Anthony, S. J., 2006. The effect of avoidance rates on bird mortality predictions made by wind turbine collision risk models. Ibis 148, 198–202.

[20] Bode, N. W. F., Franks, D. W., Wood, A. J., 2012a. Leading from the front? social networks in navigating groups. Behavioral Ecology 535 and Sociobiology 66, 835–843.

[21] Lamprecht, J., 1992. Variable leadership in bar-headed geese (anser indicus): An analysis of pair and family departures. Behaviour 122, 105–120.

[22] Kurvers, R. H. J. M., Eijkelenkamp, B., van Oers, K., van Lith, B., van Wieren, S. E., Ydenberg, R. C., Prins, H. H. T., 2009. Personality differences explain leadership in barnacle geese. Animal Behaviour 78, 447–453.

[23] Nagy, M., V., G., Pettit, B., Roberts-Mariani, I., Vicsek, T., Biro, D., 2013. Context-dependent hierarchies in pigeons. Proceedings of the National Academy of Sciences 110, 13049–13054.

[24] Leonard, N. E., Shen, T., Nabet, B., Scardovi, L., Couzin, I. D., Levin, S. A., 2012. Decision versus compromise for animal groups in motion. Proceedings of the National Academy of Sciences 109, 227–232.

[25] Richardson, T. O., Perony, N., Tessone, C. J., Bousquet, C. A. H., Manser, M. B., Schweitzer, F., 2014. A framework for extracting pairwise coupling information during collective animal motion. ArXiv e-prints 1311.1417.

[26] M Moussaïd, N Perozo, S Garnier, D Helbing, G Theraulaz (2011) The walking behaviour of pedestrian social groups and its impact on crowd dynamics. PloS one 5 (4), e10047

[27] N Pinter-Wollman et al. (2013). The dynamics of animal social networks: analytical, conceptual, and theoretical advances. Behavioral Ecology doi: 10.1093/beheco/art047

[28] R Kumar, J Novak, A Tomkins (2010) Structure and evolution of online social networks - Link mining: models, algorithms, and Applications DOI 10.1007/978-1-4419-6515-8-13, 2010 - Springer

[29] Duncan J. Watts (2004). The "New" Science of Networks, Annual Review of Sociology, Vol. 30 (2004), pp. 243-270

[30] Desholm, M., Fox, A. D., Beasley, P. D. L., Kahlert, J., 2006. Remote techniques for counting and estimating the number of bird-wind turbine collisions at sea: a review. Ibis 148, 76–89.

[31] Plonczkier, P., Simms, I. C., 2012. Radar monitoring of migrating pink footed geese: behavioural responses to offshore wind farm development. Journal of Applied Ecology 49, 1187–1194.

[32] Pennycuick, C. J., 2008. Modelling the flying bird. Academic Press, Elsevier, London, UK.

[33] Hartley, R., Zisserman, A., 2003. Multiple view geometry in computer vision. Cambridge university press.

[34] Heppner, F. H., Convissar, J. L., Moonan, D. E., 582 J., Anderson, J. G. T., 1985. Visual angle and formation flight in canada geese (branta canadensis). The Auk 102, 195–198.

[35] Bode, N. W. F., Faria, J. J., Franks, D. W., Krause, J., Wood, A. J., 2010. How perceived threat increases synchronization in collectively moving animal groups. Proceedings of the Royal Society B: Biological Sciences 277, 3065–3070.

[36] NWF Bode, AJ Wood, DW Franks (2011). The impact of social networks on animal collective motion. Animal Behaviour 82 (1), 29-38

[37] NWF Bode, AJ Wood, DW Franks (2011). Social networks and models for collective motion in animals. Behavioral Ecology and Sociobiology 65 (2), 117-130

[38] Biro, D., Freeman, R., Meade, J., Roberts, S.J., Guilford, T. (2007). Pigeons combine compass and landmark guidance in familiar route navigation Proceedings of the National Academy of Sciences of the U.S.A. 104, 7471-7476

[39] NWF Bode, DW Franks, A Jamie Wood (2010). Making noise: emergent stochasticity in collective motion. Journal of theoretical biology 267 (3), 292-299

[40] Siemens AG, February 2014. http://www.energy.siemens.com/hq/en/renewableenergy/wind-power/offshore.htm.

[41] Healy, K., McNally, L., Ruxton, G. D., Cooper, N., Jackson, A. L., 2013. Metabolic rate and body size are linked with perception of temporal in formation. Animal Behaviour 86, 685–696.

[42] Budgey, R., 1998. Three dimensional bird flock structure and its implications for birdstrike tolerence in aircraft. Proceedings of the International Bird Strike Committee 24, 307–320.

[43] Hötker, H., Thomsen, K. M., Jeromin, H., 2006. Impacts on biodiversity of exploitation of renewable energy sources: The example of birds and bats. Tech. rep., Nature and Biodiversity Conservation Union.

[44] Masden, E. A., Haydon, D. T., Fox, A. D., Furness, W., R., Bullman, R., Desholm, M., 2009. Barriers to movement: impacts of wind farms on migrating birds. ICES Journal of Marine Science 66, 746–753.

[45] Hemelrijk, C. K., Hildenbrandt, H., 2012. Schools of fish and flocks of birds: their shape and internal structure by self-organization. Interface Focus 2, 726–737.

[46] Cook, A, S. C. P., Johnston, A., Wright, L. J., Burton, N. H. K., 2012. A review of flight heights and avoidance rates of birds in relation to offshore windfarms. BTO Research Report 618.

[47] Pendlebury, C., 2006. An Appraisal of "A Review of Goose Collisions at Operating Wind Farms and Estimation of the Goose Avoidance Rate" by Fernley, J., Lowther, S. and Whitfield, P. British Trust for Ornithology.

[48] O. Chepizhko. E. Altmann, and F. Peruani, (2013). Optimal noise maximizes collective motion in heterogeneous media. Phys. Rev. Lett. 110, 238101 (2013)

[49] Seeley, T. D., Visscher, P. K., Schlegel, T., Hogan, P. M., Franks, N. R., Marshall, J. A. R., 2012. Stop signals provide cross inhibition in collective decision-making by honeybee swarms. Science 335, 108–111.

[50] Bode, N.W. F., Wood, A. J., Franks, D.W., 2012c. Social networks improve leaderless group navigation by facilitating long-distance communication. Current Zoology 58, 329–341.

[51] MEJ Newman (2003). The structure and function of complex networks. SIAM review, 2003 - SIAM